Available online at www.sciencedirect.com
SCIENCE DIRECT®
ELSEVIER
Journal of Nuclear Materials 320 (2003) 77–84
journal of nuclear materials
www.elsevier.com/locate/jnucmat

Helium in inert matrix dispersion fuels

A. van Veen [a,*], R.J.M. Konings [b], A.V. Fedorov [a]

[a] Interfaculty Reactor Institute, Delft University of Technology, Mekelweg 15, 2629 JB Delft, The Netherlands
[b] European Commission, Joint Research Centre, Institute for Transuranium Elements, Postfach 2340, D-76125 Karlsruhe, Germany

Abstract

The behaviour of helium, an important decay product in the transmutation chains of actinides, in dispersion-type inert matrix fuels is discussed. A phenomenological description of its accumulation and release in CERCER and CERMET fuel is given. A summary of recent He-implantation studies with inert matrix metal oxides (ZrO_2, $MgAl_2O_4$, MgO and Al_2O_3) is presented. A general picture is that for high helium concentrations helium and vacancy defects form helium clusters which convert into over-pressurized bubbles. At elevated temperature helium is released from the bubbles. On some occasions thermal stable nano-cavities or nano-pores remain. On the basis of these results the consequences for helium induced swelling and helium storage in oxide matrices kept at 800–1000 °C will be discussed. In addition, results of He-implantation studies for metal matrices (W, Mo, Nb and V alloys) will be presented. Introduction of helium in metals at elevated temperatures leads to clustering of helium to bubbles. When operational temperatures are higher than 0.5 melting temperature, swelling and helium embrittlement might occur.

1. Introduction

For the transmutation of actinides several fuel types are being considered: homogeneous (solid solutions) and dispersion (composite) fuels, in which an inert matrix is used as support for the actinide phase(s) [1]. Such inert matrix fuels must be designed to accommodate high helium concentrations and radiation damage. In a dispersion fuel the helium and the radiation damage are concentrated in and around the actinide phase. In general it is accepted that during irradiation to the required high burn-up the actinide particles will loose their integrity because the chemical composition changes drastically and the concomitant accumulation of gaseous fission products (fission is the actual actinide destruction process) and helium will lead to excessive pore or bubble formation as well as to cracking. The surrounding inert matrix might preserve its chemical and mechanical stability because only a small shell around the embedded particle is affected by radiation damage and implantation by helium and fission products. If care is taken that the dispersed oxide spheres are kept separated, still sufficient material that is only exposed to neutron and γ radiation will remain. However, it is expected that the actinide spheres will act as pressure centres in the inert matrix and when the fission gases and helium remain confined to the particle, they will form bubbles and eventually cause macroscopic cracking. A proper choice of the inert matrix might ensure that such mechanical failure is not occurring. However, thermal gradients and thermal cycling, as secondary effects, could lead to macroscopic damage and failure.

Many dedicated experiments have been carried out to learn about the fuel behaviour. The series of EFTTRA irradiations is an example of the concerted effort to study in-pile behaviour of inert matrix fuel [2]. Most attention has been given to the well-known CERCER fuel where actinide oxides are embedded in an oxide matrix, e.g. MgO, $MgAl_2O_4$, or other metal oxides [3]. Also, separate effect experiments have been carried out on laboratory scale to study in detail the radiation damage effects of fission or decay products [4,5] by implantation of the inert matrix with helium or other ions.

* Corresponding author. Tel.: +31-15 2782801; fax: +31-15 2786422.
E-mail address: avveen@iri.tudelft.nl (A. van Veen).

0022-3115/03/$ - see front matter © 2003 Published by Elsevier Science B.V.
doi:10.1016/S0022-3115(03)00173-9

Contrary to CERCER fuels much less attention has been given to the use of CERMET fuels. An attractive aspects of a metal matrix is the higher effective fuel thermal conductivity leading to lower fuel temperatures at the same heat load of the fuel (Fig. 1). White et al. [6], and Williams [7] invested a considerable effort in dispersion fuels for uranium dioxide. In general rather good properties were found for the metals Mo, Al, and steel as dispersion host. Their materials contained about 25 wt% of UO_2 which ensured that the particles were separated sufficiently so that the zones around the oxide particles which are damaged by fission products do not overlap. Dehaudt et al. [8] reported recently on the in-pile irradiation behaviour of molybdenum-UO_2 CERMET fuel and concluded good adhesion properties of the oxide–metal interface after irradiation. Temperatures (centre line) varied from 350 to 550 °C when the linear power was varied from 200 to 350 W cm^{-1}. Annealing to 1580 and 1700 °C revealed bubbles at the interface. At that temperature 12% of the fission gas ^{85}Kr was released. Konings and Haas [9] discussed CERCER and CERMET inert matrix fuels in general, and gave an outline of the technological aspects regarding the application of these fuels. An overview of candidate materials for CERCER and CERMET fuels is given in a recent report on advanced fuel cycles for ADS systems [10].

In this article the focus will be on helium behaviour in CERCER and CERMET fuels in which the actinide phase has a size of 50–250 μm. An attempt will be made to describe the transport properties and clustering behaviour of the helium in the inert matrix at the operation temperatures of the fuel during its lifetime. Important for the helium evolution in the fuel are the sources of helium generation, the damage rates caused by neutrons and fission products, and the temperature. Results of laboratory and reactor experiments will be reviewed. The discussion will be started with estimates of the size of the affected zones around the oxide. Preliminary laboratory experiments will be presented on helium in an inert matrix consisting of molybdenum. The effects of helium in neutron-irradiated metals have been widely studied for a variety of metals and alloys that had been candidate as first wall materials for fusion reactors. These results and Thermal Helium Desorption Spectrometry (THDS) results will be used to predict helium clustering and swelling effects in above metals at operation temperatures of 600–800 °C.

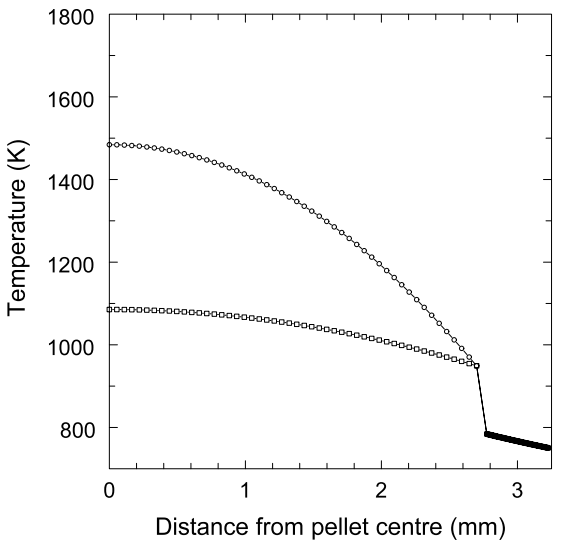

Fig. 1. Fuel temperature profiles for a CERCER composite with MgO matrix (○) and a CERMET composite with Mo matrix (□). The calculation was performed for a pellet with 5.4 mm diameter, a diametrical gap of 150 μm filled with He at 5 bar pressure at room temperature, a coolant temperature of 723 K, and a maximum linear heating rate of 280 W cm^{-1}.

2. Radiation damage and helium concentration profiles in dispersion fuels

In the 1950s the effects of fission product and α particle implantation in dispersion type fuels have already been discussed, see e.g., [6,7]. In the dispersion fuel four zones with different damage behaviour have to be considered (Fig. 2):

(i) The oxide particle with very high displacement damage. The temperature of the oxide particle will be lower for CERMET than for CERCER dispersions. This means that damage evolution can be different. In addition to damage, gaseous fission products are generated as well as helium from α decay of actinides in the transmutation chain. The outer shell of the particle is partly depleted from fission products because of recoil implantation of the

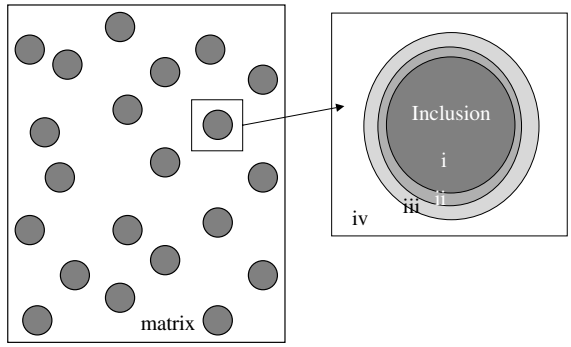

Fig. 2. Scheme of the damage levels caused by fission products and fast α's produced by an actinide or fuel particle of about 100 μm embedded in an inert matrix.

fission particles into the surrounding matrix. A simple approach is to assume that the fuel particle with radius R is gradually depleted from fission products in the shell ranging from $R - \lambda_f$ to R and enriched in the surrounding matrix from R to $R + \lambda_m$ where λ_f and λ_m are the average recoil ranges in the fuel and matrix, respectively.

(ii) The zone of about 5 μm in the host matrix around the particle, which have received a large irradiation dose of recoil implanted fission products and energetic α particles emerging from the oxide particle. Moreover, gases thermally released from the particle might accumulate at the interface. The damage might exceed 100 dpa.

(iii) A zone stretching some 13 μm away from the particle where α particles have been implanted.

(iv) The host material not affected by fission fragments or α particles. This zone is damaged by energetic neutrons alone.

Nowadays, predictions of damage and concentration profiles of helium and fission products can be rather easily be obtained by SRIM calculations [11].

Due to integration over the uniform and isotropic sources of fission products and helium in the fission particle, the profiles of damage and implanted particles are all linear decreasing functions stretching from R to $R + \lambda_m$. Fission products have typical energies of 67–95 MeV and average mass 100 amu and the helium 5–6 MeV. In a matrix with density of 10 g cm^{-3} the range of 70 MeV fission products is typically 5.5 μm and for He 13.5 μm, respectively. Fig. 3 gives a schematic overview of the ranges that might be expected. The recoiling α emitting atoms have a range of about 30 nm (for α's of 5 MeV). This gives rise to atomic mixing in a small layer.

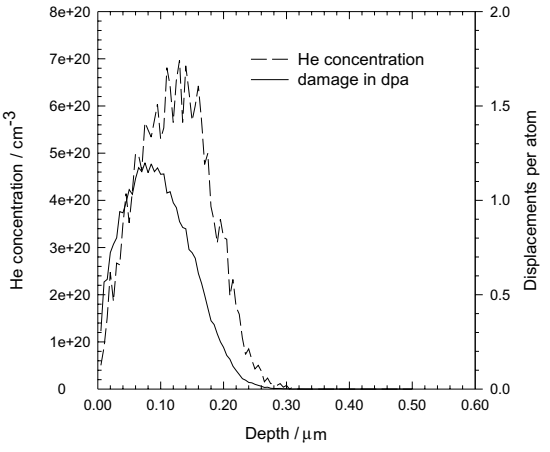

Fig. 3. Damage and helium depth profile for 30 keV He implanted into molybdenum. The fluence amounted to 10^{16} cm^{-2}.

But this is a minor effect compared to the depletion effect by the fission products and therefore can be neglected.

3. Gas assisted damage processes

Several sources are available where information can be found on damaging processes in the different zones of the composite fuel:

1. Starting in the 1950s, a major effort has been put into fast neutron radiation damage studies of metals for fusion applications. The studies have been dealing with high energy neutrons, simulating the effect of 14 MeV neutrons, to very high dpa levels. Molybdenum, tungsten, vanadium alloys and various steels have been tested to very high (>10 dpa, displacement per atom) levels at different temperatures. Void swelling has been identified as an important issue. For fusion applications care was taken to introduce also helium to levels expected from transmutation. This information is to some extent applicable to zone (ii) through (iv). In the host matrix the most severe damage conditions will be found in zone (ii). In fact it depends strongly on the particle size and distribution, but for the dispersed particles considered here (see Fig. 2) zone (iv) is only exposed to neutron damage.
2. Basic processes of gas defect complex evolution in metals have been studied by TDS. Van Veen [12] has reviewed the helium defect interactions in metals and silicon. Results are given for the evolution and thermal stability of helium–vacancy complexes in Mo, W, Cu, Au, Ni, and 316L steel. Later work includes helium in niobium and in vanadium alloys [13,14]. In general, helium when implanted at elevated temperature will form helium vacancy complexes, which can grow to bubbles. The stability of bubbles in most metals is very high. Small bubbles can migrate by surface diffusion, but larger ones are rather immobile and survive temperatures of $0.7T_m$ (melting point).
3. The EFTTRA experiments provide information on damage in the oxide particles and on the damaging effect of ions on the matrix. The EFTTRA-T3 results for macroparticles of UO_2 in various matrices showed no evidence for structural damage to the matrix but mechanical effects and accumulation of gases at the particle–matrix interface were observed [15]. The EFTTRA-T4 results for microparticles americium oxide in magnesium aluminate spinel have been described by Konings et al. [3] and Wiss et al. [16]. It was found that after irradiation in the HFR (360 full power days) the spinel matrix was structurally modified significantly and that the swelling of the fuel (18 vol.%) was linked to accumulation of helium in pores. Since ceramics are much more sensitive to fast

neutron irradiation than a metal no significant matrix effects are expected for metals. Heavy fission fragments with tens of MeV energy will damage zone (ii) to a depth of 5–10 μm dependent on the mass density of the metal. The helium implantation in zone (ii) will extend to a maximum range of 10 to 20 μm depending on the mass density of the metal. From the fission rate and decay rate of the actinides (americium) it can be derived how much fission fragments and helium are generated.

4. In the SUPERFACT experiment [17] (Am, Np, U)O_2 fuel with 20% Am + 20% Np was irradiated in the breeder reactor Phenix. The flux was 5.8×10^{15} n cm^{-2} s^{-1}. After 360 EFPD's the maximum dose was 52 dpa for the cladding. In the experiment the following gas release was measured: Xe + Kr 150 cm^3 with ratio Kr/total = 0.09 and release rate 60%. The released helium amounted to 225 cm^3 with helium 60 cm^3 STP retained. From the 97.52 g fuel oxide mass (= about 10 cm^3) it can be derived that 9×10^{20} He per cm^3 of fuel is produced. In fact, the production is about 0.5–1 fission atom and 1 He per Am.

4. Estimation of damage rate and helium production rate in zone (ii)

In zone (ii) implantation of fission products produced in the particle takes place. From EFTTRA-T4 the production of fission atoms can be taken. There are two main groups of dominant fission products: one consisting of Zr, Mo, Ru, Pd and the other one Xe, Cs, Ce and Nd. The volume concentrations based on 95% burn-up are of the order of 1×10^{21}cm^{-3} for these elements. In total 1.14×10^{22} fission products are formed. Some of them can be easily dissolved in the host metal, others will form oxide precipitates (Zr) or be insoluble (Xe, Cs). In a recent report by Konings [18] the mol fractions for Xe + Kr (0.112), Mo (0.0489), and Cs (0.0364) are quoted. The maximum range of the fission products is 5 μm if it is assumed that the initial energy amounts to 70 MeV. Each fission projectile displaces in the matrix about 4×10^4 metal atoms. Since the fission atoms start in all directions a part of them will never reach the matrix, for the particle size here considered (Fig. 2; about 100 μm), and also fission atoms starting from a distance larger than 5 μm from the oxide–matrix interface will not be stopped in the matrix. Detailed calculations can be made of the fission atom distribution across the interface but in a crude approximation it may be assumed that a zone of 5 μm adjacent to the interface will be implanted and modified. For nearly complete burn-up of the actinides, present in a concentration of 28% in the macro-dispersed fuel, the main fission products will reach concentrations of the order of a few at.%. Thus the composition of the layer is strongly modified and moreover the displacement level will be very high (>1000 dpa). The displacement rate will be of the order of 1×10^{-4} dpa s^{-1}. The continuous displacements of atoms will cause that all defect processes, like diffusion, clustering, segregation, and coalescence will be enhanced by the radiation. In spite of the relatively low temperature of the fuel (500–800 °C) this will lead to attaining quasi-thermal equilibrium states of the defects and bubbles corresponding to much higher temperatures under neutron irradiating conditions.

Helium is formed by decay after transmutation and will reach a fraction of 0.49 of the Am atoms. The energy of the helium produced by decay of the actinide isotopes is about 6 MeV. In molybdenum the maximum range at this energy will be 12 μm into the matrix. About 200 displacements are created by the helium ion. Roughly a layer of 6 μm will show a helium concentration which might exceed 20 at.%. Thus helium bubbles will be formed.

5. Helium and defects in zone (iii) and the matrix

In the zone between the matrix and the zone where the fission products are implanted only the implanted helium and displacements caused by the helium are present. In addition a similar displacement damage level is created in zone (iii) and in the matrix by the neutrons. Total displacement levels will be tens of dpa in both zones. Depending on the matrix material helium will be transported and might form small bubbles. In Sections 7 and 8 the transport and agglomeration for different materials will be discussed.

6. Gas induced mechanical effects

An important question is where the formed helium and the heavier noble gas atoms Kr and Xe will be accommodated and what mechanical effects this will induce in the dispersion fuel. For oxide particles which contain 1×10^{22} Am cm^{-3}, e.g. in (Zr, Am) O_{2-x}, in an inert oxide host, accumulation of all the helium generated by fully burn-up of the Am from a sphere with radius 50 μm will result in 5×10^{15} He in a volume of 5×10^{-7} cm^3. This corresponds to a pressure of about 40 MPa at room temperature if all the volume was available. For a open porosity of 10% created by the high damage level in the particle the pressure would be 400 MPa. The swelling of the particle is caused by defects and atoms introduced by the transmutation and fission of the cations in the oxide particle. Generally, fission leads to two new atoms, which usually have a less strong binding than the original cation. Moreover, a

considerable fraction consists of the noble gases and noble metals that have no binding at all. Furthermore helium is produced during the decay of transmuted actinides. The creation of fission products doubles the volume of the original fissionable cations and the noble gas atoms can give rise to considerably more swelling when the noble gas atoms aggregate into bubbles. Single noble gas atoms incorporated in the matrix occupy a volume comparable to that of a monovacancy of the oxide. However, when the noble gas atoms agglomerate into bubbles, considerably more volume is required to reduce the bubble pressure which is acquired by loop punching processes (plastic deformation) or by thermal creep. Pressures of noble gases in small bubbles (nm size) have been found to be in the GPa range and correspond to noble gas volume densities which are only 2–5 times lower than atomic densities of the oxide. When inter-bubble fracture occurs, the pressure will be lowered and the volume will increase. An increase of the volume with 10% will according to Eshelby's expression $P = 4/3\mu\Delta V_h/V_h$ already induce stresses in the surrounding matrix, with shear modulus μ, of the order of 0.13μ which is close to the theoretical shear strength $\mu/2\pi$. Thus the matrix will be already in an early stage subject to plastic deformation or to (inter-particle) fracture. Dependent on the temperature, thermal creep will occur. However, the creep process might be considerably enhanced by the production of radiation defects. In metals thermal creep will occur at $T > 0.5T_m$ and because of the neutron damage in the matrix some irradiation assisted creep will occur, lowering the temperature required for creep. But, if creep occurs, also fission products might diffuse into the matrix material causing a retarding effect on the creep process. Creep will be dependent on the metal or ceramics chosen for the inert matrix. Metals with low melting point, e.g. steel, vanadium will show creep at $T = 900$ K, whereas Mo, Nb, and W will not show creep phenomena at this temperature. The latter metals will also keep the helium located in small helium bubbles, and therefore no helium embrittlement phenomena will occur at the grain boundaries of the metal matrix. Relaxation will in that case occur by plastic deformation.

7. Helium transport and retention in oxides

A number of implantation experiments in candidate matrix oxides have been carried out to study the helium transport and thermal stability of helium defect complexes. The oxides MgO, Al_2O_3, (Ytrria stabilized) ZrO_2 and spinel $MgAl_2O_4$ have been implanted with 30–100 keV helium ions. For MgO and Al_2O_3 single crystals were used, for ZrO_2 sintered polycrystalline samples, and for $MgAl_2O_4$ both single crystalline as well as polycrystalline samples. Doses were varied between 1×10^{15} and 3×10^{16} cm^{-2}. However, in the case of spinel also a high energy was used 5 MeV (α's from ^{241}Am) at a very low dose of 1×10^{12} cm^{-2}, and an intermediate energy of 900 keV from implantation with an accelerator. Monitoring of the helium occurred by two techniques:

1. Neutron Depth Profiling (NDP), a technique based on the measurement of the energy distribution from the reaction of ^{3}He with thermal neutrons: ^{3}He(n,p)^{3}T. From the energy loss suffered by the monoenergetic MeV proton the depth of the helium can be calculated. ^{3}He must be used as the implanted ion.
2. Thermal Helium Desorption Spectrometry (THDS). The release rate of helium is measured when the sample is heated isochronally (typical 0.1–1 K/s). From the release rate vs temperature transients the desorption kinetics can be determined.

In Table 1 the temperature ranges (ΔT) are given in which helium release is observed. For details is referred to the references given in the table. The release temperatures ($T_{1/2}$) vary considerably depending on the sample oxide. The highest release temperature is measured for Al_2O_3 at 1750 K. By positron annihilation techniques and photon absorption it is observed that during annealing first relatively small helium vacancy complexes form (10–20 He). These release excess vacancies at $T = 1500$ K and form helium bubbles that are in thermal equilibrium. At 1750 K helium dissociates from the bubbles, and is dissolved in the matrix. Then, the bubble cavity shrinks by emission of vacancies. Once helium is trapped in bubbles it moves hardly until the dissociation temperature is reached. This is in contrast to the helium release from MgO, where bubbles are formed like in Al_2O_3. However, when the bubbles release helium, the cavities do not shrink. The release from $MgAl_2O_4$ is similar to that from MgO. There is clear evidence that in polycrystalline spinel helium release is delayed compared to single crystal $MgAl_2O_4$. This is ascribed to retrapping of the released helium in pores (closed porosity), e.g. at grain boundaries. Release from ZrO_2 takes place at rather low temperature. The transport of helium appears to be enhanced considerably by the presence of structural (compensating) vacancies in the fluorite structure. The vacancies facilitate helium to jump from one interstitial position to the adjacent one via the oxygen vacancy. For high concentrations bubbles are formed which extend the temperature range of release considerably.

8. Helium retention in metal matrices

Candidate metal hosts are Mo, W and steel (e.g. 316L) or Nb, V, Ti, Zr metals, the latter being more reactive regarding chemical interactions with oxygen,

Table 1
Helium release temperatures for helium implanted metal oxides

Sample	Structure	Depth (μm) Peak concentration (at.%)	$T_{1/2}$ (K) ΔT (K)	Remarks	Reference
MgO	Cub. monocr.	0.16 5%	1250 100	Dissociation from cavities	[19]
Al_2O_3	Hex. monocr.	0.2 0.20–5%	1750 100	Bubble shrinkage	[20]
$MgAl_2O_4$	Cub. monocr.	0–10 3×10^{-8}%	1650 400	Single helium transport	[21]
$MgAl_2O_4$	Cub. monocr.	2 0.3%	1100 200		[22]
$MgAl_2O_4$	Cub. polycr.	2 2.3%	1300 300	Retrapping in pores	[22]
ZrO_2 Y-stabilized	Cub. polycr.	0.75 0.1%	700 50	Oxygen vacancy assisted	[4]
ZrO_2 Y-stabilized	Cub. polycr.	0.75 1%	850 300	Helium in bubbles	[4]
ZrO_2 Y-stabilized	Cub. polycr.	0.15 0.5%	600 50	Oxygen vacancy assisted	[23]

hydrogen and nitrogen. In the past a considerable research effort has been devoted to helium behaviour in metals of importance for fusion reactor development. Similar conditions are present in the metal matrix of CERMET fuels as in fusion reactor wall materials. Concepts that have been applied to reduce swelling, or reduce the incubation time for swelling can be applied here. Implantation experiments in the past have been carried out to investigate transport of helium, and the nucleation and growth of helium vacancy complexes. In an overview, made in 1990, release temperatures of helium vacancy complexes in Mo, W, Ni, and 316 L are given [12]. Fedorov et al. [13,24] have published on helium vacancy complexes in vanadium and vanadium alloys. They performed also measurements on helium defect complexes formed when the implantation was carried out at elevated temperature. In general, small helium vacancy complexes are formed at low implantation temperatures. The nucleation and growth evolves via helium trapping at monovacancies and subsequent trapping of additional vacancies and helium. In Table 2 the temperatures where helium defect complexes

Table 2
Dissociation temperatures[a] (in K) of defect complexes in metals and metal alloys

Metal/T_m	$T_{melting}$	HeV(X[b])	$He_nV(X)$	He_nV_m, $m > 1$	He_n + precipitates/extended defects	Helium bubbles	Reference
W	3650	1500	1000–1200	1800		2000–2500	[12]
Mo	2880	1150	800–920	1400		1580–2100	[12,25]
Ni	1728	910	710 ($n = 2$)	1200		1400	[12]
$FeCr_{17}Ni^{13b}$	1700		730 ($n = 2$)	1070	400–900		[12]
SS 316L[b]	1700			950–1300	400–900	>1400	[12]
V[b]	2163	570	570	710–1000		1420	[13,14]
VCr_4Ti^{4b}	2100	570	570	700–1100	1350[c]	1420	[13,23,24]
Nb[b]	2741	740	600 ($n = 4$)	750–1200			[14]

Helium vacancy complexes are indicated by numbers of helium and vacancies. Helium bubbles are agglomerates with more than 100 He.

[a] The approximate temperature is indicated for dissociation while ramp heating with 1–10 K/s.

[b] The helium vacancy complexes are decorated with X = oxygen in V and Nb or other impurities (C,N).

[c] Pre-existing traps bind helium strongly in vanadium alloys.

dissociate are summarized for different metals and metal alloys. It can be seen that HeV complexes in vanadium and vanadium alloy are rather unstable. This is caused by co-trapping of He and V at dissolved oxygen positions. Helium irradiation for temperatures larger than 600 K already leads to suppression of nucleation. Instead, helium will be released to grain boundaries or be trapped in pre-existing traps. In the V–Ti–Cr alloy such precipitates bind helium clusters to rather high temperatures. Bubbles are seen to be stable close to melting point in Ni and in the austenic steel alloys.

If the helium vacancy complex is not stable at the implantation temperature helium will move until another stable trap is found, e.g. pre-existing traps at precipitates or grain boundaries. Thereby the nucleation and growth is suppressed. It is of interest to note that impurities may lower trapping of helium in vacancies because of co-trapping with the impurities. A computer program MODEX has been developed to simulate nucleation and growth of defect complexes of helium at a certain implantation temperature, and the effect of thermal treatments carried out after the implantation [25]. Good agreement has been shown with experimental desorption results for helium implanted in molybdenum.

From the earlier mentioned literature on helium in metals the following is concluded. When the temperature approaches $0.5T_m$ (T_m = melting temperature) thermal vacancies are generated and the existing helium vacancy complexes will be in thermal equilibrium with the stationary vacancy and helium concentration. Therefore helium vacancy complexes with excess numbers of vacancies (voids) will shrink. On the other hand, it will mean increased mobility of small complexes and growth of larger complexes if sufficient helium is present. Once equilibrium helium bubbles are formed in metals they are stable until high temperatures of about $0.8T_m$.

In choosing a proper metal host it is important whether the operation temperature is lower or higher than $0.5T_m$. Below $0.5T_m$ helium induced swelling might occur but stable impurity or precipitate related vacancies might delay swelling, since the helium will stay dispersed and will not be available to form the nuclei for void growth. Above $0.5T_m$ swelling is suppressed but helium bubbles might accumulate at grain boundaries and cause embrittlement. As an example, for an operation temperature of 700 °C, 316L steel will be $> 0.5T_m$ and molybdenum $< 0.5T_m$.

In order to investigate the effects of helium introduced into a real matrix material made from sintered Mo powder (produced by ITU, Karlsruhe) experiments were done as follows:

1. 30 keV He ions were implanted to a fluence of 10^{16} cm^{-2} in 15 mm diameter Mo disks made from sintered material.
2. Implantation temperatures were varied from RT to 800 °C.
3. Pieces of 0.3×0.3 cm^2 were cut and put in the crucible of a THDS apparatus for recording the release during isochronal annealing of 100 K/60 s.

The results of TRIM calculations on the helium and damage profile in Mo are shown in Fig. 2. The concentration at the peak maximum corresponds to 1 at.% and damage level is about 1 dpa. THDS results obtained for the RT and 800 °C implantation are shown in Fig. 4. The room temperature results shown in Fig. 4(a) are typical for high dose helium implantation reported

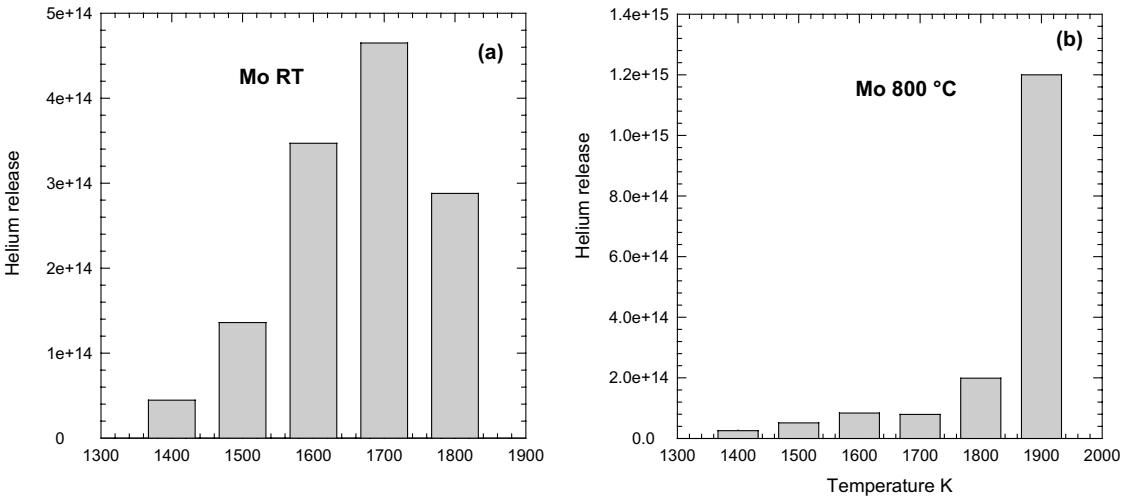

Fig. 4. Thermal helium release from 30 keV 10^{16} cm^{-2} helium ion implanted molybdenum samples: (a) implantation at room temperature (RT) and (b) implantation at 800 °C.

before for keV implanted helium. During the ramp annealing the small helium vacancy complexes dissociate at moderate temperature. Some of the helium is released, but the majority is re-trapped and forms small bubbles, which release in the temperature interval from 1500–1800 K. The desorption after implantation at 800 °C shown in Fig. 4(b) demonstrates a quite different behaviour. Apparently, small helium vacancy complexes and bubbles are not nucleated. Instead, the implanted helium has been trapped in stable pre-existing traps. It is likely that pre-existing pores in the grains and at the grain boundaries have collected the helium. Therefore, very high desorption temperatures are observed.

9. Conclusions and final remarks

A survey has been made of the phenomena that can be encountered when helium is generated in dispersion type inert matrix fuel, in particular when it concerns actinide containing particles. From point of view of helium release it seems that there is a large variation in helium mobility in the proposed metal oxides. Zirconia offers the highest helium mobility and alumina the lowest. High mobility might lead to fewer but larger helium bubbles. In addition also other elements (fission products and actinides) might have unwanted higher mobility. In metallic host matrices it is of importance whether the operation temperature is lower or higher than 0.5 melting temperature. This temperature separates different modes of mobility and defect nucleation. Below, small helium bubbles will be homogeneously nucleated and grow. Beyond, nucleation is suppressed and helium bubbles will nucleate heterogeneously in pre-existing traps. By an implantation experiment in sintered Mo it has been shown that an operation (implantation) temperature of 800 °C leads to suppression of small bubbles. Instead, very stable large bubbles are formed, releasing helium at 1600 °C.

In general, it will be expected that helium somehow will be trapped. Helium release from the fuel, which requires travel over long distances will only occur for certain oxides that allow helium permeation through the matrix, or for matrices which fail under the extreme pressures exerted by the irradiated dispersion particles. Creation of conditions for (irradiation enhanced) thermal creep might prevent release of helium and the fission gases.

References

[1] C. Degueldre, J.M. Paratte, J. Nucl. Mater. 274 (1999) 1.
[2] R.J.M. Konings, K. Bakker, J.G. Boshoven, H. Hein, M.E. Huntelaar, R.R. van der Laan, J. Nucl. Mater. (1999) 84.
[3] R.J.M. Konings, R. Conrad, G. Dassel, B.J. Pijlgroms, J. Somers, E. Toscano, J. Nucl. Mater. 282 (2000) 159.
[4] P.M.G. Damen, Hj. Matzke, C. Ronchi, J.-P. Hiernaut, T. Wiss, R. Fromknecht, A. van Veen, F. Labohm, Nucl. Instrum. and Meth. B 191 (2002) 571.
[5] E.A.C. Neeft, R.P.C. Schram, A. van Veen, F. Labohm, A.V. Fedorov, Nucl. Instrum. and Meth. B 166&167 (2000) 238.
[6] D.W. White, A.P. Beard, A.H. Willis, Irradiation Behaviour of Dispersion Fuels, US AEC TID 7546 (1957) 717.
[7] J. Williams, Dispersion Type Fuel Elements Based on Fissile Ceramics, US AEC TID (1957) 554.
[8] Ph. Dehaudt, A. Mocellin, G. Eminet, L. Caillot, G. Delette, M. Bauer, I. Viallard, IAEA Technical Committee Meeting on Research of Fuel Aimed at Low Fission Gas Release, Moscow, Russia, 1–4 October 1996.
[9] R.J.M. Konings, D. Haas, C. R. Physique 3 (2002) 1013.
[10] R.J.M. Konings (Ed)., Advanced Fuel Cycles for Accelerator-driven systems: Fuel Fabrication and Reprocessing, Report EUR 19928 EN 2001.
[11] J.F. Ziegler, J.P. Biersack, U.L. Littmark, The Stopping Power and Range of Ions in Solids, Pergamon, New York, 1985.
[12] A. van Veen, in: S.E. Donnelly, J.H. Evans (Eds.), Fundamental Aspects of Inert Gases in Solids, NATO ASI Series B, Physics, vol. 279, Plenum, New York, 1991, p. 41.
[13] A.V. Fedorov, A. van Veen, A.I. Ryazanov, J. Nucl. Mater. 258–263 (1998) 1396.
[14] H. Eleveld, PhD thesis 1996, Delft University of Technology;
M. Clement, Master thesis 1993, Delft University of Technology;
G. Buitenhuis, Master thesis 1994, Delft University of Technology.
[15] E.A.C. Neeft, K. Bakker, R.P.C. Schram, R. Conrad, R.J.M. Konings, J. Nucl. Mater., these Proceedings. doi:10.1016/S0022-3115(03)00176-4.
[16] T. Wiss, R.J.M. Konings, C.T. Walker, H. Thiele, J. Nucl. Mater., these Proceedings. doi:10.1016/S0022-3115(03)00174-0.
[17] C. Prunier, F. Boussard, L. Koch, M. Coquerelle, Nucl. Technol. 119 (1997) 141.
[18] R.J.M. Konings, J. Nucl. Sci. Technol. (Proceedings Actinides-2001), J. Nucl. Sci. Technol. (Suppl. 3) (2002) 682.
[19] A. van Veen, H. Schut, A.V. Fedorov, F. Labohm, E.A.C. Neeft, R.J.M. Konings, Nucl. Instrum. and Meth. B 148 (1999) 768.
[20] M.A. van Huis, A. van Veen, F. Labohm, to be published.
[21] E.A.C. Neeft, R.P.C. Schram, A. van Veen, F. Labohm, A.V. Fedorov, Nucl. Instrum. and Meth. B 166&167 (2000) 238.
[22] E.A.C. Neeft, A. van Veen, R.P.C. Schram, F. Labohm, Prog. Nucl. Energy 38 (2001) 287.
[23] P.M.G. Damen, A. van Veen, F. Labohm, H. Schut, presented at IMF 2002, Japan.
[24] A.V. Fedorov, Thesis, Delft University of Technology, Delft, 2000.
[25] A.V. Fedorov, A. van Veen, Comput. Mater. Sci. 9 (1998) 309.